Structures and thermodynamics of the mixed alkali alanates

J. Graetz,[1] Y. Lee,[2] J. J. Reilly,[1] S. Park,[2] and T. Vogt[2]
[1]*Department of Energy Sciences and Technology, Brookhaven National Laboratory, Upton, New York 11973, USA*
[2]*Department of Physics, Brookhaven National Laboratory, Upton, New York 11973, USA*
(Received 20 January 2005; revised manuscript received 10 March 2005; published 27 May 2005)

The thermodynamics and structural properties of the hexahydride alanates ($M_2M'AlH_6$) with the elpasolite structure have been investigated. A series of mixed alkali alanates (Na_2LiAlH_6, K_2LiAlH_6, and K_2NaAlH_6) were synthesized and found to reversibly absorb and desorb hydrogen without the need for a catalyst. Pressure-composition isotherms were measured to investigate the thermodynamics of the absorption and desorption reactions with hydrogen. Isotherms for catalyzed (4 mol% $TiCl_3$) and uncatalyzed Na_2LiAlH_6 exhibited an increase in kinetics, but no change in the bulk thermodynamics with the addition of a dopant. A structural analysis using synchrotron x-ray diffraction showed that these compounds favor the $Fm\bar{3}m$ space group with the smaller ion (M') occupying an octahedral site. These results demonstrate that appropriate cation substitutions can be used to stabilize or destabilize the material and may provide an avenue to improving the unfavorable thermodynamics of a number of materials with promising gravimetric hydrogen densities.

DOI: 10.1103/PhysRevB.71.184115 PACS number(s): 82.60.−s, 61.10.Nz, 61.66.Fn, 82.60.−s

I. INTRODUCTION

There is currently much interest in the development of a sustainable hydrogen storage material for mobile applications. The key requirements for any candidate material for practical on-board hydrogen storage are a high gravimetric hydrogen density and safe, fast and fully reversible hydrogenation near ambient conditions. Conventional metal hydrides that can readily supply hydrogen at room temperature have storage capacities <2 wt % and cannot satisfy this need. However, a number of complex hydrides have appreciable gravimetric hydrogen storage capacities, such as the sodium alanates, which reversibly absorb/desorb hydrogen with the addition of a metal dopant.[1,2] At present,there is considerable interest in understanding the kinetic enhancements attributed to the transition-metal dopant[3–5] and the mechanism by which the dopant makes the sodium alanates reversible.[6–12] The reversible hydrogenation of $NaAlH_4$ occurs in two steps in the presence of Ti:

$$3NaAlH_4 \leftrightarrow Na_3AlH_6 + 2Al + 3H_2\ (3.7\ \text{wt}\ \%), \quad (1)$$

$$2Na_3AlH_6 \leftrightarrow 6NaH + 2Al + 3H_2\ (1.9\ \text{wt}\ \%). \quad (2)$$

While the atomic mechanism is not understood, it appears that Ti resides in an under-coordinated environment at or near the surface of the depleted material.[10,13] Despite the recent attention, sodium aluminum hydride is unlikely to meet the requirements necessary for automotive applications.[14] A few alternatives that exhibit higher hydrogen capacities are $LiAlH_4$ (7.9 wt %) and $Mg(AlH_4)_2$ (6.9 wt %), which have initial hydrogen desorption temperatures of 453 K and 423 K, respectively.[5,15] However, these materials have low reaction enthalpies and therefore require extremely high pressures for the absorption of hydrogen.

Despite the unfavorable thermodynamics, it may be possible to change the decomposition temperature and pressure of the high capacity alanates by altering the material composition. The possibility of mixing two different alkali metals (M and M′) to form a mixed alanate of $M_xM'_{1-x}AlH_4$ or $M_{3-x}M'_xAlH_6$ has been explored by recent computational studies.[16,17] These efforts suggest that the tetrahydride alanates may be relatively unstable with respect to cation mixing. An *ab initio* study by de Dompablo and Ceder has shown that $Na_{1-x}Li_xAlH_4$ favors phase separation at 0 K for $0<x<1$.[17] However, there are a number of stable mixed compounds predicted for the hexahydrides, specifically the elpasolites $M_2M'AlH_6$.[16] The mixed alkali elpasolites do not revert, according to reaction (1), to a mixed tetrahydride ($M_xM'_{1-x}AlH_4$) or a mixture of monoalkali alanates ($2MAlH_4+M'AlH_4$). Rather, the absorption/desorption of hydrogen occurs in a single step analogous to reaction (2):

$$M_2M'AlH_6 \leftrightarrow 2MH + M'H + Al + \frac{3}{2}H_2. \quad (3)$$

Despite the number of predicted stable elpasolite phases, Na_2LiAlH_6 is the only composition that has been studied experimentally.[1,18] The substitution of a Li ion for a Na ion in Na_3AlH_6 to form Na_2LiAlH_6 lowers the equilibrium H_2 pressure by 20 bar at 484 K.[1] However, little else is known about the effects of alkali substitutions in the hexahydrides. In this study, the structural and thermodynamic properties of the elpasolites ($M_2M'AlH_6$ where $M\neq M'$) were investigated and compared with those of the cryolites ($M=M'$) to better understand the thermodynamic changes induced by cation mixing. Thermodynamic values were obtained by measuring pressure-composition isotherms and estimating the enthalpy and entropy of the reaction.

II. EXPERIMENTAL

Preparation of the bialkali alanates is accomplished using a number of conventional methods such as dry milling[19] or wet chemical techniques.[1,20] In this study, a tetrahydride alanate was mechanically alloyed with the appropriate alkali hydride(s) using either of the following two reactions:

$$M'AlH_4 + 2MH \rightarrow M_2M'AlH_6, \quad (4)$$

$$MAlH_4 + MH + M'H \rightarrow M_2M'AlH_6. \quad (5)$$

Precursors of $LiAlH_4$ (95%) and LiH (99.4%) were purchased from Alfa Aesar, while NaH (95%) and $NaAlH_4$ (90%) were obtained from Aldrich. KH was received from Fluka dispersed in mineral oil at a concentration of 35%. The oil was removed via an octane wash under Ar gas and dried under a vacuum. It should be noted that dry KH is extremely pyrophoric and should only be handled in an inert atmosphere. Milling was performed in an Ar atmosphere with a Fritsch Pulverisette 6 planetary mill. The gas pressure and temperature were monitored during milling to ensure that the majority of the hydrogen remained in the solid. The powders (1–2 g) were milled in a 250 mL stainless steel vial with seven 15 mm diameter stainless steel balls (13.7 g) for up to 40 h at 200 rpm. The Ti-doped material was prepared by milling 96 mol % Na_2LiAlH_6 with 4 mol % $TiCl_3$ (Aldrich) under the same conditions for 1 h.

Structural properties were determined using synchrotron x-ray diffraction (XRD). These experiments were performed on beamline X7A at the National Synchrotron Light Source of Brookhaven National Laboratory. Prior to the diffraction study, each sample was annealed for approximately 20 h under high pressure H_2 gas (160 bar at 510 K for Na_2LiAlH_6, 40 bar at 570 K for K_2NaAlH_6 and 150 bar at 480 K for K_2LiAlH_6). After annealing, the powders were sieved using a 400 mesh screen (37 μm) and then sealed in 0.5 mm glass capillary tubes under Ar gas. The capillary was mounted on the second axis of the diffractometer. A monochromatic beam was selected using a channel-cut Si(111) monochromator. A gas-proportional position-sensitive detector (PSD), gated at the Kr-escape peak, was employed for high-resolution ($\Delta d/d \sim 10^{-3}$) powder diffraction data measurements.[21] The PSD was stepped in 0.25 deg intervals between 10 deg and 70 deg in 2θ with an increasing counting time at a higher angle. The capillary was spun during the measurement to provide better powder averaging.

Pressure-composition isotherms were measured using a Sievert's-type apparatus. The material was reacted in a stainless steel tube, which was heated using a resistive tape. The internal sample temperature was monitored using a type K thermocouple. The absorption/desorption isotherms were measured by adding/removing an aliquot of H_2, allowing equilibrium to be reestablished, and measuring the pressure change.

III. RESULTS AND DISCUSSION

A. Li_2NaAlH_6 and Li_2KAlH_6

The preparation of Li_2NaAlH_6 was attempted using two different synthesis routes: reactions (4) and (5). In both cases, a characterization of the reaction products using x-ray diffraction showed the formation of a small amount Na_2LiAlH_6, but no other compositional changes. Similarly, attempts to synthesize Li_2KAlH_6 using reaction (5) were also unsuccessful. X-ray diffraction after milling revealed a reaction product consisting of $KAlH_4$ and LiH. These results suggest that Li_2NaAlH_6 and Li_2KAlH_6 are thermodynamically less stable than other competing cryolite or elpasolite phases. Lovvik *et al.* have predicted the enthalpy changes associated with mixing different alkali metals to form a bialkali alanate at 0 K using density functional theory (DFT). The large, positive mixing enthalpies associated with Li_2NaAlH_6 and Li_2KAlH_6 (10.9 and 20.8 kJ/mol, respectively) are additional evidence that these compounds are thermodynamically unstable.[16]

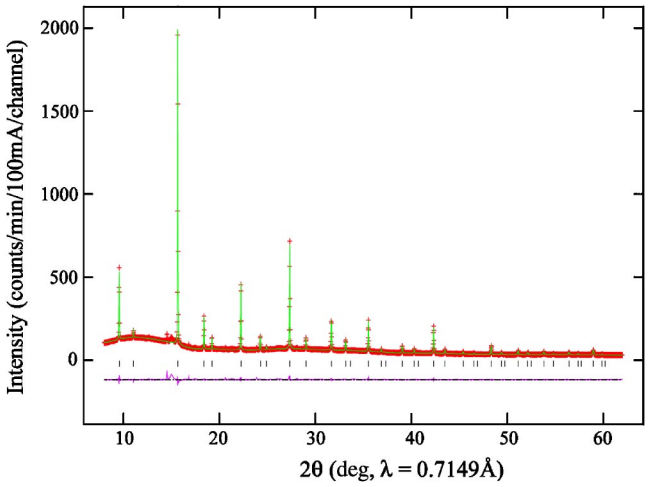

FIG. 1. (Color online) Synchrotron x-ray powder diffraction pattern from Na_2LiAlH_6 (+) showing the Rietveld fit (solid), peak positions (|), and difference pattern (below). The quality values for the Rietveld fit and weighted fit are Rp=1.90% and wRp=3.12%, respectively.

B. Na_2LiAlH_6 and Na_2KAlH_6

Na_2LiAlH_6 was prepared by both reactions (4) and (5). A characterization of the material at different stages of alloying using XRD showed that in reaction (5) intermediate phases of $NaAlH_4$ and LiH are formed before the final product (Na_2LiAlH_6), while pathway (4) leads to Na_2LiAlH_6 directly. The structure of Na_2LiAlH_6 was determined by x-ray powder diffraction using a wavelength of 0.7149 Å (Fig. 1). An elemental analysis, measured with an inductively coupled plasma-mass spectrometer (ICP-MS), confirmed a near-stoichiometric composition of 2.02:1.06:1.00 for Na:Li:Al. A Rietveld structure refinement[22,23] using GSAS[24] was performed with the constrained stoichiometry (Na_2LiAlH_6) and revealed the best fit in the $Fm\bar{3}m$ space group with a lattice constant of 7.4064(1) Å . This is in contrast with the room temperature phases of the pure cryolites Li_3AlH_6 and Na_3AlH_6, which crystallizes in the $R\bar{3}$[28] and $P2_1/n$[30] space groups, respectively. The Rietveld fit along with a difference plot are shown in Fig. 1. The results of the Rietveld analysis, displayed in Table I, demonstrate that the Na ions are in a 12-fold coordination while the Li ions occupy octahedral sites. These values are consistent with the predictions of Lovvik *et al.*[16] and are also in agreement with the space group and lattice constant reported by Claudy *et al.* using conventional x-ray diffraction.[20]

TABLE I. Interatomic distances and coordination numbers for Na_2LiAlH_6.

Neighbors	Distance (Å)	Coordination
Na-H	2.6205(3)	12
Na-Al	3.2071(1)	4
Na-Li	3.2071(1)	4
Na-Na	3.7032(1)	6
Li-H	1.952(8)	6
Li-Na	3.2071(1)	8
Li-Al	3.7032(1)	6

The pressure-composition isotherms for catalyzed and uncatalyzed Na_2LiAlH_6 are displayed in Figs. 2(a) and 2(b), respectively. Desorption isotherms are shown at various temperatures between 476 K and 518 K. The isotherms exhibit a sharp transition upon desorption, indicating the emergence of a new phase with little or no solid solution region. Another sharp transition appears at the end of desorption, indicating the depletion of the Na_2LiAlH_6 phase. A complete absorption/desorption isotherm taken at 486 K is also displayed in Fig. 2(a). The complete isotherm exhibits little hysteresis, as previously reported by Bogdanovic *et al.*[1] The

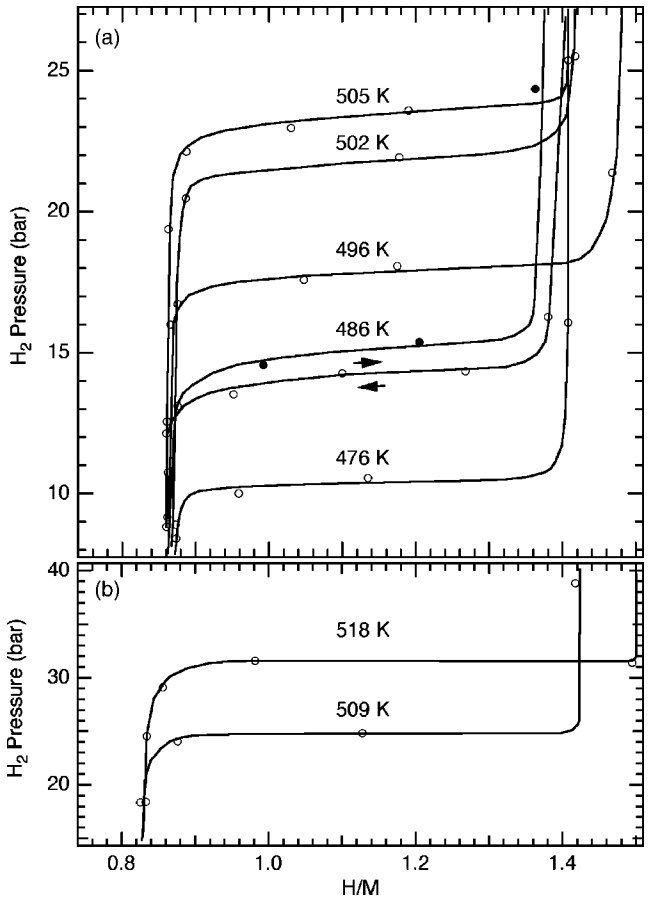

FIG. 2. Pressure-composition absorption (●) and desorption (○) isotherms for (a) Ti-doped Na_2LiAlH_6 and (b) uncatalyzed Na_2LiAlH_6. The arrows indicate the direction of hydrogen transfer.

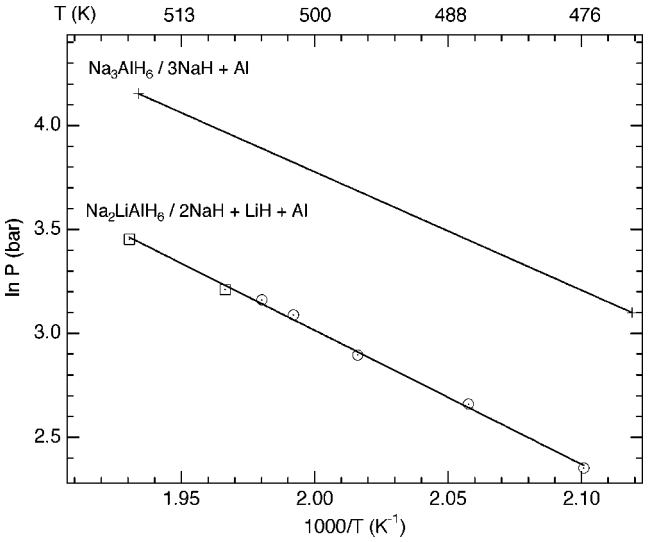

FIG. 3. Van't Hoff plot for the reversible dissociation of Ti-doped Na_3AlH_6 (+)[2] and Na_2LiAlH_6 (○—4 mol % $TiCl_3$, □—undoped).

measured hydrogen capacities for the catalyzed material are approximately 3.0 wt % (85% of theoretical) for the first cycle (496 K) and 2.6 wt % (75% of theoretical) for subsequent cycles. The hydrogen capacity for the uncatalyzed material is 3.2 wt % (91% of theoretical) for the first cycle (518 K) and 2.8 wt % (80% of theoretical) for subsequent cycles. In both cases, the capacity loss after the first cycle is attributed to incomplete absorption, which was confirmed by the presence of NaH, LiH, and Al in XRD patterns after rehydriding.

The thermodynamic parameters of the decomposition reaction were calculated from the van't Hoff equation:

$$\ln P = \frac{1}{T}\left(\frac{-\Delta H}{R}\right) + \frac{\Delta S}{R}, \tag{6}$$

where P is the equilibrium H_2 pressure at temperature T and R is the universal gas constant. Using a plot of $\ln P$ vs $1/T$, known as a van't Hoff plot, the enthalpy (ΔH) and entropy (ΔS) are determined from the slope and intercept, respectively. The van't Hoff plots for Ti-doped Na_3AlH_6[2] and Na_2LiAlH_6 (doped and undoped) are shown in Fig. 3. The equilibrium pressure values were taken from the midpoint of the plateau in Fig. 2. The plateau pressure of Na_3AlH_6 is approximately 20 bar higher than that of Na_2LiAlH_6 at 486 K and 30 bar higher at 518 K. The measured decomposition enthalpy, $\Delta H = 53.5 \pm 1.2$ kJ/mol H_2, is slightly more positive than the decomposition enthalpy of Na_3AlH_6 (47 kJ/mol H_2[2]). The entropy change, $\Delta S = 132.1 \pm 2.4$ J/mol K of H_2, is approximately equivalent to the entropy associated with the formation of molecular hydrogen [$S(H_2) = 130.7$ kJ/mol K].

The addition of a catalyst (4 mol% $TiCl_3$) significantly improves the reaction kinetics. In the uncatalyzed state, Na_2LiAlH_6 begins slowly desorbing hydrogen at approximately 490 K, while the catalyzed material exhibits a desorption temperature of less than 470 K. Similarly, the time re-

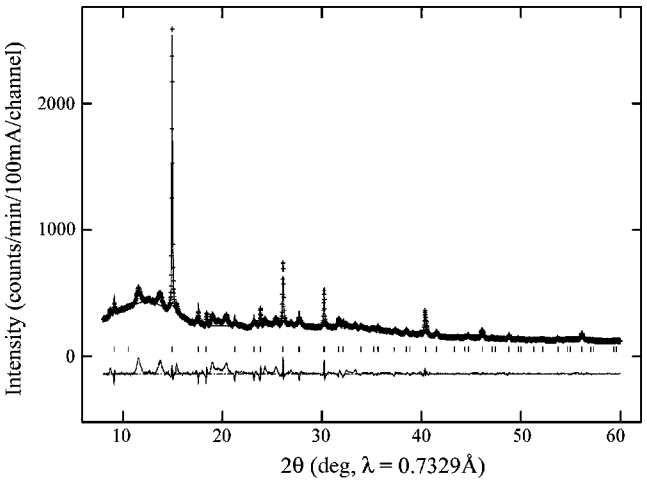

FIG. 4. Synchrotron x-ray powder diffraction pattern from K_2LiAlH_6 (+) showing the profile fit (solid), peak positions (|), and difference pattern (below). The quality value for the Lebail fit profile is wRp=5.86%.

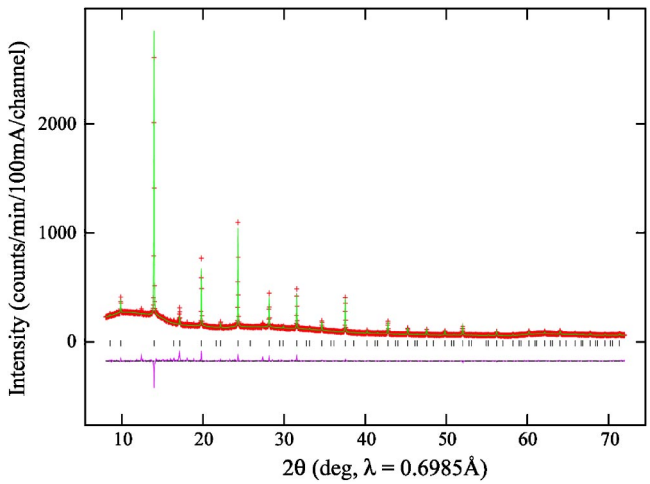

FIG. 5. (Color online) Synchrotron x-ray powder diffraction pattern from K_2NaAlH_6 (+) showing the Rietveld fit (solid), peak positions (|), and difference pattern (below). The quality values for the Rietveld fit and weighted fit are Rp=2.05% and wRp=3.08%, respectively.

quired for the system to return to equilibrium is substantially decreased by the addition of a catalyst. Equilibrium times ranged from one to two days for the Ti-doped samples to approximately one week for the undoped material.

Although the kinetics of reaction (3) are clearly enhanced by the addition of Ti, the thermodynamics remain unaffected. This is demonstrated in Fig. 3, which illustrates that the data for the catalyzed and uncatalyzed material fall on the same line in the van't Hoff plot. The dopant has no measurable effect on the enthalpy or entropy of the desorption reaction. This supports a number of recent studies that suggest that the Ti acts as a true catalyst (possibly in the form of a Ti-Al alloy)[10,11,25] and does not alter the reaction thermodynamics.

The preparation of Na_2KAlH_6 was attempted using reaction (5). X-ray diffraction of the reaction product revealed phases of K_2NaAlH_6 and Na_3AlH_6. This is consistent with predicted mixing enthalpies, which suggest that Na_2KAlH_6 is considerably less stable than K_2NaAlH_6 (by 40 kJ/mol) at 0 K.[16] Therefore, Na_2KAlH_6 should favor phase separation into equal parts K_2NaAlH_6 and Na_3AlH_6, as empirically observed.

C. K_2LiAlH_6 and K_2NaAlH_6

A new alanate was prepared by mixing K and Li ions in reaction (4) to form K_2LiAlH_6. An elemental analysis of the product (ICP-MS) revealed a near-stoichiometric composition of 2.04:1.10:1.00 for K:Li:Al. The powder diffraction results, using xrays of wavelength 0.7329 Å, are shown in Fig. 4. This pattern was not suitable for a Rietveld analysis due to a number of additional broad peaks attributed to KH impurities. However, a full profile fit to the data[26] demonstrated the best fit in the $Fm\bar{3}m$ space group with a lattice parameter of 7.9383(5) Å. As observed for Na_2LiAlH_6, the mixed potassium/lithium elpasolite crystallizes in a different space group than the pure cryolite phases Li_3AlH_6 and K_3AlH_6, which have rhombohedral[28] and tetragonal[31] symmetries, respectively. The full profile fit along with a difference pattern are displayed in Fig. 4. The $Fm\bar{3}m$ space group is consistent with the structure predicted by DFT for K_2LiAlH_6[16].

K_2NaAlH_6 was prepared by both synthesis routes [reactions (4) and (5)). The structural characterization was performed by XRD using a wavelength of 0.6985 Å (Fig. 5]. An elemental analysis (ICP-MS) gave a composition of 1.54:0.97:1.00 for K:Na:Al. A small amount of NaH was detected in the diffraction pattern, indicating that the product was probably stoichiometric K_2NaAlH_6 with a NaH impurity (~20 mol %). A sample prepared with excess KH (~25 mol %) resulted in a similar diffraction pattern, with the exception of small amounts of KH impurities. Therefore, the Rietveld refinement using the data presented in Fig. 5 was performed with a fixed stoichiometry of K_2NaAlH_6 (impurities were ignored). The Rietveld fit, in the $Fm\bar{3}m$ space group, along with a difference plot, are shown in Fig. 5. The measured lattice parameter is a=8.1209(1) Å. The nearest-neighbor distances and coordination numbers are listed in Table II.

The first and only other reported synthesis of K_2NaAlH_6 used reaction (4) in an organic medium under high pressure (25 kbar) H_2 gas. An XRD structural characterization of this

TABLE II. Interatomic distances and coordination numbers for K_2NaAlH_6.

Neighbors	Distance (Å)	Coordination
K-H	2.8841(3)	12
K-Al	3.5164(1)	4
K-Na	3.5164(1)	4
K-K	4.0604(1)	6
Na-H	2.3027(27)	6
Na-K	3.5164(1)	8
Na-Al	4.0604(1)	6

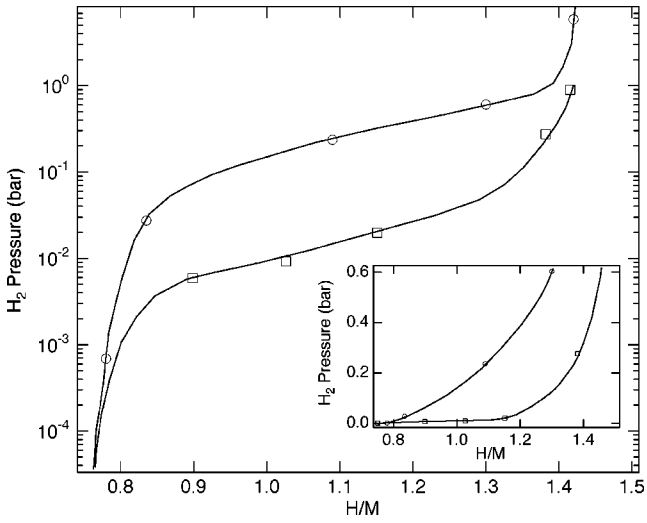

FIG. 6. Pressure-composition absorption isotherms (no doping) for K_2NaAlH_6 (○) and K_2NaAlH_6 (□) at 574 K plotted on a semilog scale. A plot of the data on a linear scale is displayed in the inset.

material suggested a monoclinic unit cell with dimensions $a=5.706$ Å, $b=5.707$ Å, $c=8.114$ Å, and $\beta=90.24$ deg.[27] The discrepancy in the structural parameters may be attributed to the high pressure synthesis used in the earlier study, which may have distorted the unit cell from the cubic $Fm\bar{3}m$ structure.

The pressure-composition absorption isotherms for K_2LiAlH_6 and K_2NaAlH_6 at 574 K are shown in Fig. 6. The initial desorption occurs at approximately 500 K for K_2LiAlH_6 and 530 K for K_2NaAlH_6. At 574 K, the absorption reaction proceeds slowly in both samples. The time required for the system to reach equilibrium after the addition of H_2 gas is around 280 h for K_2LiAlH_6 and greater than 1000 h for K_2NaAlH_6. Both isotherms exhibit a gradual increase in equilibrium pressure with respect to composition. The lack of a clearly defined pressure plateau indicates that these materials do not exhibit a definitive two phase region at 574 K. It is likely that these data were collected at a temperature above the critical temperature of the miscibility gap in the compositional phase diagram. The measured hydrogen storage capacity for K_2LiAlH_6 and K_2NaAlH_6 is 2.3 wt % and 2.0 wt %, respectively. This capacity is ~90% of the theoretical value and the loss is attributed to an impurity of KOH in the KH precursor.

Due to the impractically slow reaction kinetics, it was not feasible to measure a series of desorption isotherms at different temperatures. Therefore, the reaction enthalpies for K_2LiAlH_6 and K_2NaAlH_6 were approximated from Eq. (6). The equilibrium pressures were taken from the midpoint of the isotherms shown in Fig. 6. The entropy was estimated, $\Delta S|_{T\to\infty}\approx 130.7$ kJ/mol K, using the change in entropy associated with the transition of hydrogen from an ordered solid to a gas. The estimated decomposition enthalpies [reaction (3)] for K_2LiAlH_6 and K_2NaAlH_6 are 82 kJ/mol H_2 and 97 kJ/mol H_2, respectively.

A summary of the structural and thermodynamic data for the hexahydride alanates is presented in Table III. The bialkali alanates have a face centered cubic structure in the $Fm\bar{3}m$ space group, similar to the high temperature (525 K) sodium alanate phase, β-Na_3AlH_6.[33] In these compounds (β-$M_2M'AlH_6$), the smaller M′ is octahedrally coordinated while M has a 12-fold coordination. A diagram of the general elpasolite structure is shown in Fig. 7. In the monoclinic ($P2_1/n$) polymorph, α-$M_2M'AlH_6$, the M ion is coordinated by eight atoms.[34] *Ab initio* calculations have predicted α-Na_2LiAlH_6 to be slightly more stable than the β-phase at 0 K.[17] However, at 300 K the experimental data suggests that the β polymorph is preferred for all of the stable bialkali alanates. It is interesting to note that when two different alkali metals are present, the octahedral site is always occupied by the smaller ion. The compounds Li_2NaAlH_6, Li_2KAlH_6, and Na_2KAlH_6 tend to phase separate, suggesting that the substitution of the smaller ion into the 12-fold coordinated site is thermodynamically unfavorable. This trend also seems to apply to the "true" elpasolites, $M_2M'AlF_6$. Each of the

TABLE III. Structural and thermodynamic properties based upon experimental data for alanates of the form $M_2M'AlH_6$. The parameters listed include the structure (space group or symmetry), lattice constants, decomposition enthalpy (ΔH) and decomposition temperature (T_d). The data for the cryolite phases were obtained from the references listed.

M	M′	Structure	Lattice constants (Å)	ΔH (kJ/mol H_2)	T_d (K)	References
Li	Li	$R\bar{3}$	$a=8.0712(1)$, $c=9.5130(2)$	43.5	453	28, 29, and 15
	Na	Unstable	-	-	-	
	K	Unstable	-	-	-	
Na	Li	$Fm\bar{3}m$	$a=7.4064(1)$	53.5(12)	490	
	Na	$P2_1/n$	$a=5.390(2)$, $b=5.514(2)$ $c=7.725(3)$, $\beta=89.86(3)$ deg	47	473	30, 2, and 1
	K	Unstable		-	-	
K	Li	$Fm\bar{3}m$	$a=7.9383(5)$	82	500	
	Na	$Fm\bar{3}m$	$a=8.1209(1)$	97	530	
	K	tetragonal	$a=8.445$, $b=8.584$	135	593	31, 32, and 27

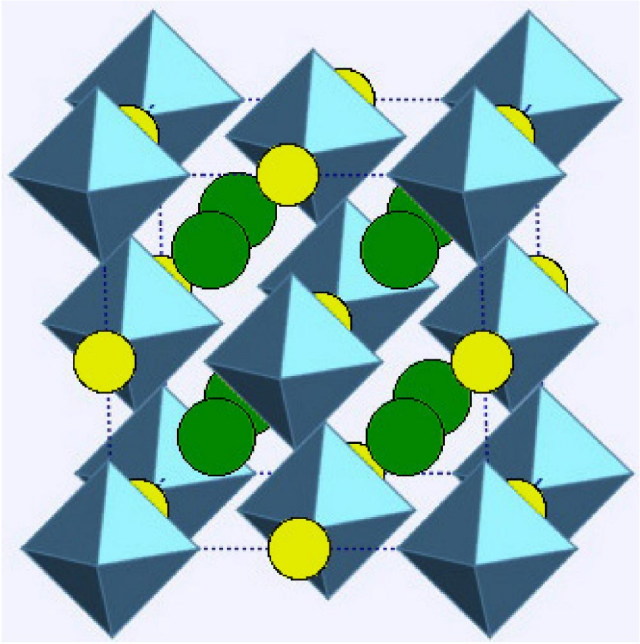

FIG. 7. (Color online) Structural diagram of $M_2M'AlH_6$ showing AlH_6 octahedra, M cations (large) and M′ cations (small).

stable bialkali aluminum hydrides (M,M′=Li, Na, or K) has a corresponding fluoride compound with a similar lattice constant (±0.2 Å)[35–37] in the $Fm\bar{3}m$ space group. Analogous to the hydrides, there are no reported fluorides where M′ is greater than M.

The decomposition temperature (T_d) and enthalpy are also dependent upon the size of the alkali metals M and M′. The substitution of Li for Na to form Na_2LiAlH_6 increases ΔH and T_d by 6.5 kJ/mol and 20 K, respectively. This case is an exception to the general rule that the decomposition temperature and enthalpy increase with the size of the alkali metal. This trend is well documented for the monoalkali alanates, as shown in Table III. The tendency for greater hydride stability with a larger alkali metal also applies when only a partial substitution of the metal is involved. For example in the K-M′ alanates, K_2NaAlH_6 is 14.6 kJ/mol more stable than K_2LiAlH_6 and 38.5 kJ/mol less stable than K_2KAlH6.

IV. CONCLUSION

Novel elpasolite phases of the complex alanates were synthesized using conventional mechanical alloying techniques. Each of these compounds reversibly absorbs and desorbs hydrogen without a catalyst. The addition of a catalyst to Na_2LiAlH_6 shows improved kinetics, but no change in the bulk thermodynamics. Structural analyses of the bialkali alanates demonstrates that the preferred space group is $Fm\bar{3}m$, with the larger ion in a 12-fold coordination and the smaller occupying an octahedral site. In general, a smaller alkali ion (M or M′) reduces the reaction enthalpy of the hexahydride. These results demonstrate that the temperature of hydrogen evolution and the equilibrium gas pressure can be tailored by appropriate substitutions of the alkali metals.

ACKNOWLEDGEMENTS

This work, including research carried out at the NSLS (beamline X7A), was supported by an LDRD at Brookhaven and by the U.S. DOE under Contract No. DE-AC02-98CH10886. The authors would also like to thank Santanu Chaudhuri (BNL) for his insight on the structure and stability of the mixed alanates.

[1] B. Bogdanovic and M. Schwickardi, J. Alloys Compd., **253–254** 1 (1997).
[2] B. Bogdanovic, R. A. Brand, A. Marjanovic, M. Schwickardi, and J. Tolle, J. Alloys Compd. **302**, 36 (2000).
[3] G. Sandrock, K. Gross, and G. Thomas, J. Alloys Compd. **339**, 299 (2002).
[4] T. Kiyobayashi, S. S. Srinivasan, D. Sun, and C. M. Jensen, J. Phys. Chem. A **107** 7671 (2003).
[5] M. Fichtner, J. Engel, O. Fuhr, O. Kircher, and O. Rubner, Mater. Sci. Eng., B **108**, 42 (2004).
[6] K. J. Gross, S. Guthrie, S. Takara, and G. Thomas, J. Alloys Compd. **297**, 270 (2000).
[7] D. Sun, T. Kiyobayashi, H. T. Takeshita, N. Kuriyama, and C. M. Jensen, J. Alloys Compd. **337**, L8 (2002).
[8] B. Bogdanovic, M. Felderhoff, M. Germann, M. Hartel, A. Pommerin, F. Schuth, C. Weidenthaler, and B. Zibrowius, J. Alloys Compd. **350**, 246 (2003).
[9] H. W. Brinks, C. M. Jensen, S. S. Srinivasan, B. C. Hauback, D. Blanchard, and K. Murphy, J. Alloys Compd. **376**, 215 (2004).
[10] J. Graetz, A. Yu. Ignatov, T. A. Tyson, J. J. Reilly, and J. Johnson, Appl. Phys. Lett. **85**, 500 (2004).
[11] M. Felderhoff, K. Klementiev, W. Grunert, B. Spliethoff, B. Tesche, J. M. von Colbe, B. Bogdanovic, M. Hartel, A. Pommerin, F. Schuth, and C. Weidenthaler, Phys. Chem. Chem. Phys. **6**, 4369 (2004).
[12] J. Iniguez, T. Yildirim, T. J. Udovic, M. Sulic, and C. M. Jensen, Phys. Rev. B **70**, 060101(R) (2004).
[13] J. Graetz, A. Yu. Ignatov, T. A. Tyson, J. J. Reilly, and J. Johnson, Mater. Res. Soc. Symp. Proc. **837**, N2.4.1 (2005).
[14] Hydrogen Storage Draft, in *Multiyear Research Development, and Demonstration Plan. Planned Activities for 2003-2010, US DOE Hydrogen, Fuel Cells & Infrastructure Technologies Program*. http://www.eere.energy.gov/hydrogenandfuelcells/mypp/, 2003.
[15] D. Blanchard, H. W. Brinks, B. C. Hauback, and P. Norby, Mater. Sci. Eng., B **108**, 54 (2004).
[16] O. M. Lovvik and O. Swang, Europhys. Lett. **67**, 607 (2004).
[17] M. E. A. Y. de Dompablo and G. Ceder, J. Alloys Compd. **364**, 6–12 (2004).
[18] L. Zaluski, A. Zaluska, and J. O. Strom-Olsen, J. Alloys Compd. **290**, 71 (1999).
[19] J. Huot, S. Boily, V. Guther, and R. Schulz, J. Alloys Compd. **383**, 304 (1999).
[20] P. Claudy, B. Bonnetot, J. P. Bastide, and J. M. Letoffe, Mater.

Res. Bull. **17**, 1499 (1982).
[21] G. C. Smith, Synchrotron Radiat. News **4**, 24 (1991).
[22] H. M. Rietveld, J. Appl. Crystallogr. **2**, 65–71 (1966).
[23] R. A. Young, *The RietVeld Method, International Union of Crystallography* (Oxford University Press, New York, 1995).
[24] A. C. Larson and R. B. Vondreele, *GSAS, General Structure Analysis System*. Report LAUR 86-745, Los Alamos National Laboratory, New Mexico, 1986.
[25] G. J. Thomas, K. J. Gross, N. Y. C. Yang, and C. Jensen, J. Alloys Compd. **330–332**, 702 (2002).
[26] A. Le Bail, H. Duroy, and J. L. Fourquet. Mater. Res. Bull. **23**, 447 (1988).
[27] J. P. Bastide, P. Claudy, J. M. Letoffe, and J. El Hajri, Rev. Chim. Miner. **24**, 248 (1987).
[28] H. W. Brinks and B. C. Hauback, J. Alloys Compd. **354**, 143 (2003).
[29] T. N. Dymova, D. P. Aleksandrov, V. N. Konoplev, T. A. Silina, and A. S. Sizareva, Koord. Khim. **20**, 279 (1994).
[30] E. Ronnebro, D. Noreus, K. Kadir, A. Reiser, and B. Bogdanovic, J. Alloys Compd. **299**, 101 (2000).
[31] P. Chini, A. Baradel, and C. Vacca, Chim. Ind. (Milan) **48**, 56 (1966).
[32] W. Grochala and P. P. Edwards, Chem. Rev. (Washington, D.C.) **104**, 1283 (2004).
[33] P. Claudy, B. Bonnetot, G. Chahine, and J. M. Letoffe, Thermochim. Acta **38**, 75 (1980).
[34] J. P. Bastide, B. Bonnetot, J. M. Letoffe, and P. Claudy, Mater. Res. Bull. **16**, 91–96, 1981.
[35] J. L. Holm and B. J. Holm, Acta Chem. Scand. (1947-1973) **24**, 2535 (1970).
[36] J. Graulich, S. Drueke, and D. Babel, Z. Anorg. Allg. Chem. **624**, 1460 (1998).
[37] L. R. Morss, J. Inorg. Nucl. Chem. **36**, 3876 (1974).